8

Field-Aligned Current Mechanisms of Prominence Destabilization

Petko Nenovski
National Institute of Geophysics, Geodesy and Geography, Sofia
Bulgaria

1. Introduction

Solar wind is initiated from active solar flare regions. Solar flares start with an active-region prominence: cold dense plasma associated with an arcade of looped magnetic field lines. A prominence can be stable for hours or days but sometimes it takes on a violent evolution: as the magnetic field structure slowly evolves, the loop becomes more and more stretched and the prominence starts rising slowly until the configuration becomes highly unstable and reconnection initiates, causing a large, impulsive energy release which will make the prominence erupt more rapidly; as reconnection continues both the erupting prominence and the plasma on the newly formed loops are heated tremendously causing very bright X-ray emissions. Some flares are accompanied by coronal mass ejections where plasma piled up in the corona above the rising magnetic loops is ejected by the intense energy bursts associated with reconnecting field lines. The lower-lying prominence which consists of chromospheric material might be ejected as well. Coronal mass ejections (CME) give rise to large disturbances propagating outward in the solar wind. This picture points out that prominences are a basic source of solar wind in which the Earth's and planet magnetospheres and other non-magnetized planets are continuously immersed. When emitted in a direction which brings it on a collision course with the Earth, a CME will have a profound impact on the outskirts of the terrestrial atmosphere: the magnetosphere and the ionosphere (Bellan, 2004).

Prominences are arched structures protruding from the solar surface. They are known to consist of plasma-filled magnetic flux tubes and occur at many different scales. Also, they are imbedded in a hot corona via a so-called prominence-corona transition region. Quiescent prominences (QPs) are those prominences located in the solar corona and are denser and cooler objects than their surroundings and relatively quiet if they are viewed at large time scales. Prominences invariably are located parallel to and above a photospheric, magnetic polarity reversal line, although not every part of a reversal line has a prominence above it. Polarimetric observation has shown that a prominence is threaded by a largely horizontal magnetic field with a principal component along the prominence length (Leroy 1989; Tandberg-Hanssen 1995). Therefore, prominences are naturally classified by whether their magnetic fields thread in the same or opposite direction relative to the direction of the underlying photospheric bipolar field. These two types of prominences, described as normal

and inverse, respectively, imply distinct topologies for the coronal magnetic fields around the prominence.

The precise knowledge of prominence plasma parameters (temperature, density, ionisation ratio and magnetic field) is very important for prominence theory and related problems (Tandberg-Hanssen 1995). Typical values of QP temperature lie in the range 5000-8000 K (Hirayama 1985a; Zhang et al. 1987; Mein & Mein 1991). Lower temperatures (T ~ 4300 K) have been reported by Hirayama (1985b). An interesting tendency of increasing prominence temperature toward the outer edges, where temperatures may reach values of 10^4 to $2x10^4$ K, has been pointed out by Hirayama (1971). The prominence plasma density is not as well known as the temperature because of observational difficulties. The electron density is in the range of 10^{10} –10^{11} cm^{-3} (Hirayama 1972), but these values have been found not to be precise (Vial 1986). The registered densities depend on both the prominence type and the method used (Hirayama 1985b). Electron densities ten times smaller (Bommier et al. 1986) and larger than 10^{11} cm^{-3} (N_e ~ $10^{11.3}$ cm^{-3}) (Landman 1984a) have been found. The hydrogen density of QP lies in the range of (3÷6)x10^{11} cm^{-3} (Landman 1984a; Vernazza 1981; Hirayama 1986) The ionisation ratio n_{HII}/n_{HI} usually varies in the interval of 1-3. According to Landman (1984b) it is in the range of 0.05 -1, although higher values (~3) have been obtained by Vial (1982).

The prominence magnetic field plays an important role in the QP formation, stability and dynamics. Its magnitude and orientation depend on the FAC flowing within the prominence body. The first measurements of the longitudinal component of the magnetic field (along the prominence axis) have been done by Zirin & Severny (1961) using the Zeeman effect. The results based on this effect were summarized by Tandberg-Hanssen (1995). With the use of the Hanle effect, a new technique has been developed to measure the longitudinal and transversal prominence magnetic field (Leroy 1985). The absolute magnetic field strength in the QPs is generally found to be in the range from a few Gauss to 10 G, occasionally reaching 20 or 30 G.

Another characteristic of the QPs is the presence of internal motions during their stable period, i.e. when they are not activated. The velocity field of a QP is due to three main types of motions - vertical, horizontal and oscillations. The vertical motions can be divided into two classes - downward flows and upward flows. Downward motions are registered in prominences at the limb (Engvold 1976; Cui Shu et al. 1985) and have values of about 5 kms^{-1} . Spectrographic studies (Kubot 1980) give an average value of 0.7 kms^{-1}. Upward flows of 0.5÷5 kms^{-1} are observed in disk filaments (Mein 1977; Schmieder et al. 1984; Schmieder et al. 1985). Mass flows along filament threads, with a flow velocity in the range 5-25 km s^{-1}, have also been observed (Zirker et al. 1998; Lin et al. 2003, 2005). Zirker et al. (1998) and Lin et al. (2003) have detected flows in opposite directions within adjacent threads, a phenomenon known as counterstreaming. Some observations show fast (50 kms^{-1}) horizontal motions (inclined to the axis of the prominence at about 20°) at the edges of the filaments (Malherbe et al. 1983). Usually, the velocity of horizontal motions in QP is 10 to 20 kms^{-1}.

The presence of oscillatory motions in QPs is a proven observational fact (Tsubaki 1989; Vrsnak 1993; Vrsnak & Ruzdjak 1994). A rough classification of the prominence oscillations, made on the basis of oscillation amplitude, divides them into two main classes; large amplitude (20 kms^{-1}) oscillations affecting the whole object, and small amplitude (20 kms^{-1})

oscillations affecting the fibril or a restricted area within the prominence (Oliver 1999). The oscillations may have a large range of periods - from a few minutes to hours (Bashkirtsev et al. 1983; Bashkirtsev & Mashnich 1984; Weihr et al. 1984). Some observers have detected oscillations and travelling waves in individual threads or groups of threads (Yi et al. 1991; Yi & Engvold 1991; Lin 2004; Lin et al. 2007), with periods typically between 3 and 20 minutes. The prominence fibril structure also exhibits periodic variations (Tsubaki et al. 1988); individual fibrils may oscillate with their own periods (Thomson & Schmieder 1991; Yi et al. 1991). There is also some evidence that velocity oscillations are more easily detected at the edges of prominences or where the material seems fainter than in the prominence body (Tsubaki & Takeuchi 1986; Tsubaki et al. 1988).

Recently, high-resolution images of solar filaments (e.g., Lin et al. 2003, 2005, 2007) clearly show the existence of horizontal fine-structures within the filament body. This observational evidence suggests that prominences are composed of many field-aligned *threads*. These threads are usually skewed with respect to the filament long axis by an angle of 20° on average, although their orientation can vary significantly within the same prominence (Lin 2004). The observed thickness, d, and length, l, of threads are typically in the ranges $0.2'' < d < 0.6''$ and $5'' < l < 20''$ (Lin et al. 2005). Since the observed thickness is close to the resolution of present-day telescopes, it is likely that even thinner threads could exist. According to some models, a thread is believed to be part of a larger magnetic coronal flux tube which is anchored in the photosphere (e.g., Ballester & Priest 1989), with denser and cooler material near its apex, i.e., the observed thread itself. The process that leads to the formation of such structures however, is still unknown (e.g. Lin etal, 2005;2007).

The prominence plasma is thus a complex system in terms of temperature, density, plasma motion and specific magnetic field configuration. However, if we take into account the prominence fine structure, they *must be treated as dynamic and nonhomogenous formations of field-aligned currents (FACs)*. The FAC characteristics are usually unknown and nowadays there are no methods to detect them. The FAC are intrinsically connected with the magnetic field configuration. The subject of this review is the stability problem of field-aligned currents (FAC) flowing along prominence body.

In conventional MHD theory field-aligned currents (FAC) are supported by Alfven waves. There is another source of FAC, which is primarily due to the Alfven wave gradient existing at the plasma boundaries. In addition to the Alfven modes, the MHD surface waves, supported by these boundaries, can also carry field-aligned currents. The surface wave FAC should be dislocated, either at the prominence boundaries or within the prominence body. A physical interpretation of surface wave FAC as a boundary phenomenon, i.e. as FAC flowing into the plasma boundary structures, has also been given (Nenovski 1996). The MHD surface waves have been formerly examined as a source of field-aligned electric currents and they are suggested to promote QP destabilization via a field-aligned current (FAC) intensification process (Nenovski et al., 2001). The SW can, however, carry FAC only under certain conditions. The MHD surface wave should be a non-axial mode, i.e. it has to propagate obliquely to the ambient magnetic field. The surface wave FAC propagation or the surface wave group velocity is however directed practically along the magnetic field.

These "wave induced" currents tend to be concentrated at the prominence periphery, i.e. they are surface field-aligned currents. Such currents can be intensified in the case when

surface wave bouncing processes at the prominence feet are possible and conditions for negative reflection (under negative dielectric properties conditions) are present. This surface FAC yields an increase of the azimuthal component of the magnetic field, which in turn may destabilize the whole QP system (Nenovski et al., 2001). The preferable situations for such a "switch on" of QP destabilization process require a plasma density increase at the footpoints and/or a low density plasma condition in the prominence body. The magnetic field strength requirements (threshold) depend on the neutral density variations and the neutral-plasma density ratio (Nenovski et al., 2001).

2. Intensification of the FACs, filamentation and dissipation

On the other hand, the process of wave FAC intensification if it starts will be followed inevitably by FAC density increase and hence instability due to non-linearity effects may emerge. Consequently there are various non-linear effects. The most dangerous one is the structural instability known as Bennett's pinch instability due to the interaction of the current with its own magnetic field. This is explainable by imagining the FAC as being composed of smaller individual components of that current all travelling within the prominence body, therefore a net inward pressure on the surface of this body will be generated. A further intensification of field-aligned currents could be followed by compression and distortion of plasma and ambient magnetic field at some points of the prominence body. As a consequence, the prominence structure composed by field-aligned current density and magnetic field flux where the field-aligned current flows can finally be disrupted. We advice the reader to read about the pinch effect initially examined by Northrup (1907) and also major developments by Bennett published in 1934 where an analysis of the full radial pressure balance in a static Z-pinch has been executed.

Examining in detail the field-aligned current density distribution along the prominence body the following considerations should be taken into account. First, the field-aligned currents supported by either Alfven wave, or MHD surface wave, would not occupy the whole cross section of the prominence body – hence the Bennett's instability configuration could not be realized. Second, along the flux tube coinciding with the prominence body the magnetic field flux $\Phi=B.S$ is constant, but the magnetic field intensity B would be inversely proportional to changes in the prominence cross section S. The cross section S changes along the prominence body. Therefore, the field-aligned current propagation could be followed by field-aligned current density changes (increase or decrease). Depending on the field aligned current density distribution, a field-aligned current filament mechanism would starts and be operative at points where FAC density becomes maximized.

2.1 Distribution of elementary currents

Note that a FAC structure mechanism embedded in the ambient FAC structure coexisting with the prominence is considered. Thus we will examine possible FAC structure formation process being easily initiated in the regions where the FAC intensities are sufficiently high, e.g. at the chromosphere-corona transition regions just above the chromosphere. The influence of the chromosphere on the FAC structures of course is through its conductivity (Appendix A). It is expected that pre-existing chromospheric density inhomogeneities of various scales could also influence an initiation of the FAC structure formation process. The latter are usually of irregular characteristics and probably of local extent. Initially we neglect them.

Before going to examine FAC structure mechanism by itself, let us introduce some relevant physical quantities. In previous analytical treatments of the plasma vortex structures (e.g. Southwood and Kivelson, 1993) less theoretical attention has been paid to the microphysics of the filament/vortex formation mechanism. We define the vorticity Ω by

$$\Omega \equiv \frac{\vec{B}_0 \cdot (\nabla \times \vec{v})}{B_0} \tag{1}$$

where $\boldsymbol{B_0}$ is the undisturbed magnetic field, $\boldsymbol{v}$ is the plasma velocity. Under MHD approach, three sources of field-aligned currents are known (Sato, 1982):

$$B\partial / \partial z(j_{||} / B) = \rho d / dt(\vec{B} \cdot \nabla \times \vec{v} / B^2) +$$
$$(2 / B)\vec{B} \times (\nabla P / B^2 + \rho / B^2 d\vec{v} / dt) \cdot \nabla B - \vec{B} \times (\rho / B^2 d\vec{v} / dt) \cdot \nabla N / N$$

Where v, $\rho = MN$ and P are the velocity, density and kinetic pressure of the plasma treated as MHD medium; the coordinate z is oriented along the magnetic field $\boldsymbol{B}_0$. Once a large-scale FAC is generated it flows along the magnetic field fluxes satisfying some boundary conditions. We will study effects coming from the FAC intensity changes down the magnetic field lines. The first source to the FAC intensity change is connected to the vorticity $\boldsymbol{\Omega}$ (see the first term). The second and third ones are due to gradients ∇N, ∇P, ∇B connected with the magnetic flux configurations and the inertial term dv/dt (the time derivative d/dt is equal to $\partial/\partial t + \boldsymbol{v}.d/d\boldsymbol{r}$). The time derivative d/dt is reduced to the $\boldsymbol{v}.d/d\boldsymbol{r}$ term, i.e. we should take into account velocity gradients only along the plasma flow $\boldsymbol{v}$. Thus inertial term does not contribute essentially to the large-scale FAC dynamics unless the triple scalar product $\boldsymbol{B}_0 \times (\boldsymbol{v}.d/d\boldsymbol{r})\boldsymbol{v}.\nabla B_0(N)$ yields in some cases considerable FAC input. Hence inertial term will contribute to the FAC changes only in the presence steep gradients ∇B, or ∇N (∇P). Indeed, steep gradients $\nabla B_0(N)$ are encountered at boundary crossings. The boundary regions (where FAC structures are located) by itself are however characterized with internal gradients $\nabla B_0(N)$ less than the steep gradients existing at their edges. Therefore, excluding fast time variations the vorticity $\boldsymbol{\Omega}$ appears to be main source of steady-state large-scale FAC intensity changes along the field lines. Then, performing the divergence operator on

$$\vec{E} + \vec{v} \times \vec{B} = 0 \tag{2}$$

one obtains

$$\nabla \cdot \vec{E} = -\vec{B} \cdot \nabla \times \vec{v} = -B\Omega \tag{3}$$

So

$$\Omega = -\rho / \varepsilon_0 B_0 = -eN_0 / \varepsilon_0 B_0 \tag{4}$$

where ρ is the equivalent charge density (see Parker, 1979); N_0 is the corresponding number density. This relation states that the vorticity $\boldsymbol{\Omega}$ is equivalent to a charge density ρ. Using the charge conservation condition we could connect the charge ρ with the field-aligned current $\boldsymbol{j}_{||}$: $div\boldsymbol{j} = -d\rho/dt$. The FACs actually discharge the charges (built in the FAC source regions) by carrying them along the magnetic field lines. If we neglect the magnetic field line

curvature and other gradient effects the current $j_{\perp}$ that flows perpendicular to the magnetic field lines is equal to zero (Shkarofsky et al., 1966). Therefore

$$div\vec{j} = div\vec{j}_{||} = \partial j_{||} / \partial z = -d\rho / dt \tag{5}$$

In connection to plasma convective vortex motion $\boldsymbol{v}$, the field-aligned currents could be thought of as current discharges of electric charges being accumulated in the source regions. We will here interrelate the current discharges concept with the charge formalism because the latter is well developed. Now we are looking for FAC dynamics along the magnetic field lines. There are FAC structures of zero frequency (e.g. Nenovski, 1996). The time derivative $\mathrm{d}/\mathrm{d}t$ is then given by $\boldsymbol{v}_{||}\, d/dz$, where $\boldsymbol{v}_{||}$ is the field-aligned charge velocity along the magnetic field lines. Eq. (5) relates quantitatively the field-aligned current density $\boldsymbol{j}_{||}$ and the vorticity $\boldsymbol{\Omega}$:

$$\vec{j}_{||} = \varepsilon_0 B_0 \vec{v}_{||} \Omega \tag{6}$$

It is assumed that $\boldsymbol{v}_{||}$ in eq. (6) coincides exactly with the Alfven speed v_A. The current density $\boldsymbol{j}_{||}(z)$ depends obviously on the vortex $\boldsymbol{\Omega}$ and the Alfven velocity v_A distribution. The FAC carriers are of course ions or electrons. These charges however interact to each other and therefore the FAC 'elements' ($d\boldsymbol{j}_{||}$) are subjected to the same forces as the charges. Their motion along the magnetic field lines produces in fact FAC elements of different sign. An ensemble of FAC elements with positive and negative signs (two-component ensemble) could be intervened in that supposedly possesses all the features of the classical Coulomb system of electrons and ions. Under this concept the distribution of the FAC elements is treated in terms of associated charge distribution. The accompanying plasma vortices (1) are to be consequently described by an appropriate stream function.

After having defined the vorticity $\boldsymbol{\Omega}$ and its relevance to the charge concept we need to clarify the forces of an ensemble of field-aligned currents elements $d\boldsymbol{I}$. In magnetohydrodynamics (MHD), the current elements have finite length dl. This is due to chaotic, thermal motion of the charges. Each charge does not flow continuously along the magnetic field lines thus forming an infinite current line. Instead, its trajectory along the field line is interrupted at some distance. Due to thermal motion inherent to all charges in the system, new charge appears in place of the given charge that continues the charge motion along the field lines. We assume that an ensemble of current elements, or charges, which are continuously flowing along the field lines, builds a field-aligned current of infinite length. In order to estimate quantitatively the FAC distribution, the FAC elements interaction should be examined. The field-aligned current structure of infinite length will then consist of 'bundles' of one-polarity current elements each of length dl. Indeed, it is well known that the force that these field-aligned current elements experience obeys to the Biot-Savart laws, i.e.

$$F = \frac{(dI \sin\theta) \cdot dl}{r^2} = \frac{j_{||} \sin\theta dV}{r^2} \tag{7}$$

where $dI = \boldsymbol{j}_{||}.\boldsymbol{dS}$ is the current strength of a single current element, dl ($\mathrm{d}l << r$), $\boldsymbol{dS}$ and $\mathrm{d}V = \boldsymbol{dl}.\boldsymbol{dS}$ are its length, square and volume, respectively. The angle θ denotes the angle

between the axis of the current elements and the point of field action. In the case of ensemble of current elements of opposite polarity and equal density N_0, the interaction process at very small angles θ will be screened from other current elements and then it will be less effective than in vacuum. Thus we assume that in an ensemble of current elements the interaction process takes place at angles θ nearly equal to $\pi/2$. The size of the interaction region cannot be much less than $(dV)^{1/3}$, i.e. $r > (N_0)^{-1/3}$. The square dependence on r however suggests that the description of the current element ensemble is analogous to that of the classical Coulomb system. A correspondence exists when the conventional charge in the Coulomb law stands for the charge $(j_{\|}\sin\theta)dV\sqrt{\varepsilon_o\mu_0}$ where μ_0 is the magnetic permeability. The volume element dV is expressed by the plasma density: $dV = N_0^{-1}$. For comparison with the classical Coulomb system of electrons and ions, in our case each current element is considered to be aligned along the magnetic field lines (an axial symmetry). After having determined the equivalence between the FAC elements and the charges that they carry, the FAC filament distribution appears to be e.g. a Boltzman-like. For this purpose the Biot-Savart law (7) guarantees the equivalence with the Coulomb law.

In order to understand the physics of filamentation, the field-aligned currents are examined as an ensemble of elementary currents. This allows using an approach similar to that of the spatial distribution of particles in a classical Coulomb system. According to (3) we have

$$\nabla \cdot \vec{E} = -\vec{B}_0 \cdot (\nabla \times \vec{v}) = -B_0(\Omega(+) + \Omega(-) \tag{8}$$

where Ω(+) and Ω(−) correspond to vortices densities of positive and negative signs (with respect to the undisturbed magnetic field $\boldsymbol{B}_0$). The vortex distribution could be determined by assuming a Boltzman-like distribution of the relevant single charge q $(j_{\|}\sin\theta)dV\sqrt{\varepsilon_o\mu_0} \rightarrow q$ Hence we have

$$\Omega(\pm) = \pm(^{eN_0(\pm)}/_{\varepsilon_0 B_0})\exp(^{\vec{j}_{\|}(\pm)\cdot\vec{A}}/_{N_0(\pm)\cdot\Theta}) \tag{9}$$

where $N_0(\pm)$ is the number density of the positive (negative) vortices; $\boldsymbol{A}_\infty$ is the potential of a zero 'charge' defined by $q(\boldsymbol{A}_\infty) = 0$; Θ is the Gibb's distribution module. The sum of Ω(+) and Ω(−) of course will represent the total vortex density at given point. The solar plasma system is inhomogeneous and often in a non-equilbrium state. Then, the Ω(+) and Ω(−) distributions depends on the conditions under which the system exists. The particle distributions and associated vortices Ω(±) are assumed to be stationary and take different form. In the frequent current/neutral sheets configurations where the magnetic field is nearly zero the particles obey to the Speiser's distribution (Speiser, 1965; 1967). Particle distributions adjacent to the current/neutral sheets could be modeled as isotropic ones and may be approximated by either a velocity exponential ($f \sim \exp[-(E/\varepsilon)^{1/2}]$, where E is the particle energy and ε is related to thermal energy E_T in a parametric manner ($\varepsilon = \varepsilon(E_T)$), or kappa function ($f \sim [1+E/kE_T]^{-k-1}$) instead of Maxwellian one (e.g. Christon et al., 1988). The forth-coming FAC structure formation process could be described either velocity exponential, or kappa distributions. In these cases the corresponding constants ε or E_T stands for the Gibb's module Θ, defined for equilibrium state. In a non-equilibrium state distributions Ω(+) and Ω(−) (9) will incorporate additional terms which will indicate

possible (first-order) anisotropy in the non-equilibrium FAC distribution. Further we examine disturbances Ω(+) and Ω(−) to an initial equilibrium state particle distribution, the self-interaction of current elements, $j_{//}(\pm)/N_0(\pm)$ and subsequent vortex formation processes. Their distribution will be then governed by a self-consistent vector potential ψ (Balescu, 1975), where ψ stands for $\boldsymbol{j}_{\|}(\pm).\boldsymbol{A}/N_0(\pm)$. Because the quasi-neutrality condition is fulfilled for both charges and currents in plasmas, i.e. their densities N_0**(+),** N_0**(–)** coincide, we study only configurations of equal current strength I**(±)** of both polarities, I**(±) =** I_0, We define N_0**(±) =** N_0. Our basic equation of the field-aligned current elements dI of density N_0 then reads

$$\begin{aligned} &\Delta\vec{A} + \mu_0\vec{j}_{||}\sinh(\vec{j}_{||}\cdot\vec{A}/N_0\Theta) = 0 \Rightarrow \\ &\Delta(\vec{j}_{||}\cdot\vec{A}/N_0\Theta) + (\mu_0 j_{||}{}^2/N_0\Theta)\sinh(\vec{j}_{||}\cdot\vec{A}/N_0\Theta) = 0 \end{aligned} \tag{10}$$

Here $\boldsymbol{j}_{\|}.\boldsymbol{A}/N_0\Theta =$ **(**$\boldsymbol{A}.\boldsymbol{v}_{\|}$**)** where $\boldsymbol{v}_{\|}$ coincides with the Alfven velocity $\boldsymbol{v}_{\mathrm{A}}$. The quantity $\boldsymbol{A}.\boldsymbol{v}_{\|}$ has a meaning of potential 'φ' which governs the distribution of charges q being given by (1). The coefficient λ^2 ($\lambda^2 = \mu_0(j_{\|})^2/N_0\Theta$) is proportional to the squared single charge q and charge density N_0 (Nenovski et al., 2003)

The current density $\boldsymbol{j}_{\|}$**(**z**)** depends obviously on the vortex Ω and the Alfven velocity v_A distribution (see (6)). Thus it varies along the magnetic field lines. Both quantities Ω and v_A are determined by the prominence magnetic field geometry and the plasma density distribution. The FAC flowing along a magnetic field usually occupies a flux tube of given cross section $\boldsymbol{S}$. Because the magnetic field lines are parallel to the borders, $\boldsymbol{B}_0.\boldsymbol{S} =$ constant, then the FAC intensity will increase proportionally to the magnetic field magnitude $\boldsymbol{B}_0$. For given plasma density distribution $N = N(z)$, where z is the distance, we could express the vortex Ω and the Alfven wave v_A distribution along the field lines by geometry factors $L_{1,2}(z)$. Thus $\boldsymbol{\Omega}(z) = \Omega_0 L_1(z)$ and $\mathbf{v_A}(z) = \mathbf{v_{A0}}L_2(z)$, where z_0 is a starting point, e.g. the FAC source point. Quantitatively, the basic relation that accounts for the FAC distribution along the magnetic field lines has the form

$$\vec{j}_{||}(z) = \vec{j}_{0,||}L(z/z_0) \tag{11}$$

where the geometry factor $L(z/z_0)$ can be determined observationally. Thus, due the prominence magnetic field geometry the nonlinear term in eq. (10) will steeply change its magnitude $\lambda^2(z)$. It is noteworthy to mention that this feature persists irrespective of the fact whether the FAC structure has wave, or static nature. Therefore, the FAC density increase is the principal cause of the filament/vortex formation process due to self-interaction of the FAC elements.

The existence of nonlinearity suggests a FAC structure formation process that under certain conditions generates new spatial distribution of FAC vortice (thread) structures. By solving it we obtain various solutions governing the FAC structure formation process. This enables us to determine the FAC densities needed for FAC filament formation. Let us now consider the magnitude of the coefficient $1/\lambda^2$**(**z**)** that controls the nonlinearly of our FAC system and, if possible, to obtain its actual magnitude. Before doing so, it is noteworthy to mention that eq. (10) is analogous to the nonlinear Poisson-Boltzman (PB) equation (Debye and Hueckel, 1923; Balescu, 1975)

$$\Delta\Psi = r_{De}^{-2}\sinh(\Psi) \tag{12}$$

It describes the spatial trend of the self-consistent electrostatic potential and the plasma number density. $\Psi = q(\varphi-\varphi_\infty)/kT$ is the normalized self-consistent 'electric' potential: $\boldsymbol{E} = -\nabla\varphi$; r_{De} is the Debye radius. Of course, this potential Ψ corresponds to the self-consistent electric potential in the classical Coulomb system (Ecker, 1972). Eqs. (10,12) are also identical to the Euler's equation for stationary flows of incompressible fluids (Kaptsov, 1988). It is well known also that solutions of such equations yield vortex structures of different scales. It is well known that such system possesses collective behavior, i.e. long-ranged correlative effect caused by the electric field produced by the charged particles (electrons and ions) emerges over the entire plasma system. It has already been shown that in such a system, under certain conditions periodic plasma number density distributions of some scales appear. These structures are dependent on the nonlinear term $\sinh(\Psi)$ and its coefficient, the Debye length r_{De}(e.g. Martinov et al., 1984, Martinov et al., 1986). In the derived nonlinear equation of the FAC element self-interaction (10) our coefficient λ^2 is equivalent to the squared Debye length in (12). In order to understand the physical meaning of the coefficient λ^2 let us examine the expression for the Debye length r_{De} in the classical Poisson-Boltzman equation. The latter is proportional to

$$N_0 e^2 / \varepsilon_0 kT \tag{13}$$

where e is the single charge, T the prominence temperature. In eq. (13) the $N_0 e$ quantity stands for the 'charge' density ρ where the charge e stands for $j_{II} dV\sqrt{\varepsilon_0\mu_0} = \frac{j_{II}}{N_0}\sqrt{\varepsilon_0\mu_0}$.

Because of the relationship (6), the vorticity Ω stands for this eN_0 quantity. We replace eN_0 with its equivalent q and obtain

$$N_0 q^2 / \varepsilon_0 kT = q\rho / \varepsilon_0 kT = (\varepsilon_0 / kT)(\vec{B}_0 \cdot \nabla \times \vec{v}) \tag{14}$$

It follows that the coefficient that determines the nonlinearity of the field-aligned current filament formation is determined by

$$\lambda^2 \equiv (N_0 q) / (\mu_0 j_{||}{}^2) = (cv_T / v_A)^2 / (v_A\Omega)^2 = \beta(c / v_A)^2 / (c / \Omega)^2, \tag{15}$$

where c is the light velocity, v_T the plasma thermal velocity, and β the ratio of plasma to magnetic pressure. Thus we have a fully determined coefficient needed for studying the FAC filament formation process.

Examining the physical parameters entering in (15) one can see that under given field-aligned current and vortex geometry, the filament formation process would be initiated at the minimum β value point. The smallest values of β are for 'cold' plasma, $\beta < m/M$, m and M are the electron and ion mass, respectively. It follows that the filament formation process will most easily appear at chromospheric heights. On the other hand, when the field-aligned current penetrates within corona, an increase of the FAC density $j_{||}$ (11) (by a factor z/z_0) enhances additionally the magnitude of the coefficient (15) (depending on λ^{-2}) governing the nonlinearity effect. Thus, we could suppose that at these heights the nonlinearity effect appears first. Each physical object described by such a Coulomb system

would admit different periodic spatial distributions, which yield different structures of the system.

Remind that magnetohydrodynamic equilibrium state is governed by the nonlinear equation in the form (Shafranov, 1963)

$$\Delta A = -k\frac{dP}{dA}$$

where pressure $P = p + B_{\|}^2/2\mu_0$ and P is an arbitrary functions of A ($\boldsymbol{A}$ is of course the vector magnetic potential, $p(A)$ and $B_{\|}^2/2\mu_0$ are the plasma and the magnetic field pressures) have been considered. In an equilibrium state both the plasma pressure $p(A)$ and the magnetic field $B_{\|}(A)$ determine the needed function $P(A)$. The latter determines the kind of nonlinearity which governs the vector potential distribution (Parker, 1979). The coefficient k of course characterizes the nonlinearity of the system and is an unknown parameter. In literature, several forms of the nonlinear function $G(A) = dP/dA$ have been chosen (e.g. Kriegman and Reiss, 1978; Streltsov et al, 1990). Thus we find a concordance of eq. (10) with the basic equation in magnetohydrodynamics.

2.2 Field-aligned current (FAC) filamentation instability

The above theoretical considerations represent a good basis for a simple construction of FAC filamentation process that starts at certain threshold values of the FAC density being intensified in the prominence body. It is found that the filament formation process starts at (Nenovski et al, 2003):

$$a^2 / \lambda^2 = \pi^2(4 + a^2 / b^2)$$

(λ is determined by (15) and b coincides with the size of the longer size of the rectangle of the field-aligned current localization region (a,b)). The lowest magnitude for a filament formation process is achieved at aspect ratio $r \equiv a/b \to 1$, i.e. for tube-like FAC structures. For sheet-like FAC structures the geometry ratio is high and the filament formation process is less attainable. Using eq. (10) we are able to determine the minimum 'charge' density ρ, or the field-aligned current density magnitude $j_{\|,\mathrm{crit}}$ needed for an initiation of fillament formation process. Having assumed square FAC region, the filament formation begins at (Nenovski et al, 2003)

$$j_{\|,crit}a \geq 0.63(v_T / v_{T0})\ [\mathrm{A/m}] \tag{16}$$

where v_{T0} is the plasma 'thermal' velocity that corresponds to ambient prominence temperature T_0 assumed to be equal to 1x10^4 °K. Under prominence conditions the actual temperature varies and can reach values up to 60000 °K, e.g. T_0 is between 1-6 eV. Let us evaluate qualitatively the magnetic field strength produced by such filament current. Assuming that the azimuthal magnetic field $B_{\perp}$ produced by FAC filament is proportional to the quantity $\mu_0 j_{\|} a$ and that the filament current size is obviously of thousand km and less we obtain the following critical values for the $B_{\perp}$ magnitudes: 10^{-6}-10^{-5} T. The actual magnitudes of $B_{\perp}$ are, of course, higher.

The critical current intensity depends on the current region size a (the smaller one) and therefore, it increases when a decreases. The threshold value current magnitude is controlled by the plasma 'thermal' velocity v_T of the current carriers. The newly formed FAC structures (filaments) are of scale a/m, or b/n where (m,n) characterize the number of vortices in the x and y directions. Hence, the size a in (16) should be replaced by a factor F

$$F = \frac{a}{\sqrt{m^2 + n^2 a^2 / b^2}}$$

This means that the critical (threshold) field-aligned current density $j_{||,crit}$ (m,n) will increase with decreasing FAC structure scales. Factor F is thus a measure of the FAC filaments scaling with respect to the whole size of the initial FAC structure. Note that under the Earth's magnetosphere conditions this factor can raise up to two orders, where the current density in FAC structures span the interval from μA/m² to 10^{-4} A/m² (Iijima and Potemra, 1976).

It is noteworthy to mention that the dependence of $j_{||,crit}$ on the thermal velocity can be thought as a counterpart of the Bennett's formula that states that the pinching effect of the field-aligned current is balanced by the plasma thermal pressure. The latter is however proportional to the squared thermal velocity, i.e. the threshold FAC strength (I) for pinching is proportional to v_T**.** Only in the case of *one polarity* (ambient) current I (in our examination it corresponds to $m = 1,\ n = 1$) the threshold value field-aligned current density coincides quantitatively with the Bennett formula.

A comparison of the suggested FAC structure (filaments) formation model with some observation sets of FAC structures/thread events is now possible. Remind that the ambient (large-scale) FAC structures might be hidden and that the final FAC filament/vortex structures will dominate. It follows that upward and downward FACs are generated within the ambient FAC geometry.

It is noteworthy to mention that an analogue of the examined FAC filamentation process could be found under the Earth's magnetosphere conditions (Nenovski et al 2003). There is a variety of FAC structure data which yield evidences for such a coexistence of Birkeland's FACs known also as Regions 1 (R1) and Region 2 (R2), and periodical FACs of smaller scales (Arshinkov et al. 1985; Ohtani et al. 1994). The measured FAC intensities exceed the threshold value ones (16). According to experimental results, these FAC structures are superimposed onto a larger-scale FAC system and the background FAC density measured in the FAC region 1 (R1) is three times less than the FAC sheet density of smaller scales. Taking into account that the FAC sheet intensity and thickness are correspondingly 0.2 A/m and 200 km we derive 3.33×10^{-7} A/m². This value exceeds 2.5 times the threshold value one. Hence, there are experimental evidences that the FAC filament formation process might take place.

2.3 Consequences of FAC filamentation instability

In our approach a hypothesis for a statistical distribution of FAC elements with Gibbs distribution module Θ is introduced. FAC elements governed by equilibrium-like or stationary forms of distribution are also allowed for. The considered FAC elements interact to each other in the same way as in the classical Coulomb system. For this ensemble, long-

ranged correlative effects are consequently expected. All the FAC filaments (upward and downward) yield totally zero field-aligned current that corresponds to the quasi-neutrality condition of the charges in plasmas. The negative charges (electrons) compensate the positive charges of the ions. By using a 'charge' concept of the FAC elements we derived *quantitatively* an estimate of the parameter λ^2 which stands for the non-specified coefficient k introduced in the Grad-Shafranov equation of magnetohydrodynamic (MHD) equilbria. In the 'charge' approach adopted by us this parameter (λ^{-2}) depends on the density N_0 of the FAC filaments and the thermal energy T of the dominant plasma/prominence constituent. In the plane perpendicular to the ambient magnetic field the FAC element distribution could be described as if there were no magnetic field. This assumption could be accepted as far as there are no other effects – magnetic field curvatures, inertial or drift motion, etc. The governing physical parameter is the temperature T of the plasma environment. Hence, the separation of FAC elements into FAC structures/filaments is controlled by this temperature. An increase of FAC intensity along the magnetic field lines is however the principal factor for FAC structure/thread formation that is taken into account. When the FAC travels through the chromosphere-solar corona regions the plasma temperature T and the corresponding plasma parameter β could change. Both the FAC intensity and β changes along the magnetic field fluxes will control FAC structure formation processes. Preferable conditions for the examined FAC structure formation processes are expected to be initiated at heights approaching the chromosphere-corona transition region. Therefore, the FAC filament formation due to self-interaction process is expected to be a dominant feature at heights just above the chromosphere.

2.4 FAC structures generation in inhomogeneous plasma flows

Differential movements of the photospheric footpoints of magnetic flux in the solar atmosphere are studied both experimentally and theoretically during last three decades (Wu et al, 1983). FAC structures or threads can thus be generated by such processes of differential motions embedded in the chromosphere. The shear motion in the solar atmosphere will generate non-potential magnetic field, i.e. the magnetic field is twisted (Wu et al, 1983). Experimental evidences exist which yield a power dependence between the velocity and the magnetic field localization of type $v = \alpha B^{\beta}$ ($\beta \neq 1$) (Stenflo, 1976). Observations in H_α lines of the fine structures of Quescent Prominences (QP) reveal that various twisted magnetic fluxes in the form of filaments or threads (along the QP body) exist. The arch-like QP and loops, for example, consist of one or more stable magnetic flux ropes which exist few weeks or several months. What dynamic processes are responsible for their filament formation and destabilzation? Do these filament (thread) structures untwist and disappear subsequently by changes in the external conditions? These and other similar problems are not fully modelled even in the frame of MHD. The dynamical responses to photospheric shear motions, i.e. movements of footpoints of flux tubes have numerically been examined by Wu et al. (1983). In their study a build-up of magnetic energy up to 4 times faster than the rate of other modes (kinetic, potential, etc.) is shown. The volume where the magnetic energy is growing after the introduction of the shear, is limited, the magnetic field gradient is correspondingly concentrated in a narrow slab in the vicinity of the neutral line of the shear motion (Wu et al, 1983). Wu et al (1983) have suggested these magnetic field intensification processes as a source of flare energy. The quiescent prominences (QP) is interestingly to study because of possible steady-state twisted magnetic

flux structures coexisting with the external conditions of simultaneous inhomogeneous shear flows, magnetic fields of inverse polarity and so on.

Theoretical considerations of the connection between the internal structures and the external conditions are needed. It is well-known that QPs are situated over the dark filaments (on solar disk) where the magnetic field polarity inversion and velocity shear are presented. It is possible also that the QP footpoints are subjected to both movement and rotation. It is expected that the inhomogeneity in the steady flow has to influence the structure behavior of the QP more dramatically. For example, a velocity shift at the plasma boundary can lead to the Kelvin-Helmholtz instability. Under velocity shift conditions there are always gradients and a boundary of finite extent evolves. The correct understanding of the physical processes connected with the QP internal magnetic structures requires to taking into account more explicitly the plasma and the magnetic field inhomogeneities. From theoretical point of view the finite spatial scales of the boundary inhomogeneities will induce new structures with own velocity and magnetic field characteristics. To best of our knowledge the structure formation problem in the presence of velocity and magnetic field inhomogeneities is not thoroughly examined.

2.4.1 Theoretical modeling

Consider a magnetic flux loop surrounded by inhomogeneous flow. The background magnetic field $\boldsymbol{B}$ is oriented along the z-axis. The plasma flow $\boldsymbol{V}$ can be modelled in two ways. In the first case, the inhomogeneity (the gradients) is oriented along the x-axis only (Case I), in the second one, the velocity gradient is along the radius (a cylindrical geometry)(Case II). The second case is responsible for the plasma rotation structure effects, as pointed by the well-known laboratory experiments (Nezlin et al, 1987; Nezlin and Snezhkin, 1993; Nezlin, 1994). In our opinion, theoretical consideration of flux tube structure formation suitable for the QP destabilization can simply be illustrated by Case I. Let us imagine a flux tube and choose a cross-section of some radius r_0. Denote the two ends of the tube diameter (along axis y) of this cross-section by points S and D. We consider the following plasma flow-(magnetic) flux tube geometry: An inhomogeneous flow is coming at point S, streams around the flux tube, say to the right, and drops out at point D. Another flow is coming in the cross-section from point D and goes round the rest of the flux tube on the left side and reaching point S disappears (a shear flow model). Thus, the magnetic flux is streamed entirely and its boundary of radius r_0 can be represented as a streamline. For convenience, the considered tube radius r_0 is assumed to be equal to 1 (in dimensionless presentation). The following problems are raised. Do such magnetic tubes (ropes) exist in the presence of velocity shears? Do velocity itself and its gradient cause (generate) filament structures and/or twisted magnetic (threads) inside the flux ropes?

Thus, our task is to study the internal structure evolution and stability of such tubes. We note that because the QP length L exceeds considerably the QP cross thickness we do not account for the possible differentiation along this tube length. In order to answer to these questions we study the structure formation in the presence of velocity gradients across the main magnetic field $\boldsymbol{B_0}$**.** The model consists of plasma flow $\boldsymbol{V}_0$ (along the y-axis) perpendicular to the $\boldsymbol{B_0}$. The unperturbed magnetic filed is along the z-axis but an additional component $\boldsymbol{B}_\perp$ is assumed. The $\boldsymbol{B}_\perp$ vector makes with the velocity vector V_0 an angle smaller than $\pi/2$. We assume an x-dependent velocity given as a series

$$V = V_0 + V_0^{'}x + \frac{1}{2}V_0^{''}x^2 + ... \tag{17}$$

It is convenient to examine separately possible plasma structure formation due to constants V_0, V_0' (velocity gradient) and so on. For a description of the filament (thread) formation under velocity shear conditions (17) the set of reduced magnetohydrodynamics (RMHD) is allowed for. It is known that in the RMHD case the velocity and magnetic vector potential components parallel to the background magnetic field suffice to describe the self-consitent evolution of the plasma. These potentials $\boldsymbol{\varphi}$ and $\boldsymbol{A}$ should comprise all inhomogeneity characteritics depending on (x,y) coordinates. The initial set of RMHD reads

$$\begin{aligned}
&\partial\rho / \partial t + [\varphi, \rho] = [\rho_0, \varphi] \\
&\partial / \partial t(\nabla_\perp{}^2\varphi) + [\varphi, \nabla_\perp{}^2\varphi] = \rho_0{}^{-2}[\rho, P_0] \\
&-[\rho^{-1}\nabla_\perp{}^2 A, A - B_\perp x] + B_0\nabla_\perp(\rho^{-1}\nabla_\perp \partial A / \partial x) \\
&\partial A / \partial t + [\varphi, A - B_\perp x] = B_0 \partial\varphi / \partial x
\end{aligned} \tag{18}$$

The following assumptions are inferred. The time changes are slow compared to the transit time $t_A \equiv r_{0,max}/v_A$ where v_A is the Alfven velocity: $((\partial/\partial t)^{-1} > O(t_A))$; the z-changes are comparable to time changes $(v_A\partial/\partial z)^{-1} \approx (\partial/\partial t)^{-1} < t_A{}^{-1})$; the plasma parameter β ($\beta \equiv 2\mu_0 P/B^2$) is assumed small. Following the Strauss analysis (Strauss, 1977) the flow velocity should be considered as incompressible and of course perpendicular to the background magnetic field. In seeking localized in (x,y) plane solutions of (18) a proper motion of the modes along the y-axis as assumed, i.e. $\partial/\partial t = -u\partial/\partial y$. The derived mode structure is inclined at angle ϑ to the undisturbed magnetic field $\boldsymbol{B_0}$, ($\tan\vartheta \equiv B_0/B_\perp$).

Let us now study separately three cases a) V_0 = const; b) $V_0 = 0$, but $V_0' \neq 0$ (a shear). Later on, $V_0 \neq 0$, and $V_0' \neq 0$ are considered. In the first case the set basic equations (18) reduces to

$$(1 - m^2\mu_0{}^{-1}\rho^{-1})\Delta(\varphi_0 - V_0 x) = \pm k^2(\varphi_0 - V_0 x) - px \tag{19}$$

where a linear dependence between φ_0 and A is allowed ($A_0 = m\varphi_0$) and a coefficient p which cumulates the terms due to the perpendicular magnetic field $\boldsymbol{B}_\perp$ and constant pressure gradient ∇P is introduced. The coefficients m is equal to $B_\perp/V_0$. In the case of uniform flow V_0 a dipole (modon) structure, is possible (Strauss, 1977). Note that under uniform velocity conditions (V_0 = const, $V_0' = 0$) interesting six-cell type (Nenovski, 2008) structures are possible. In the latter case a dipole structure of smaller size still exists in the centre and four-cell, sheet-like structures of various sizes which surround the central structure appear (Nenovski, 2008). Note that the dipole structure is only a vestige and the four-sheet features of the cells dominate. Note also that the field-aligned currents (FAC) supported by the such a structure formation are of inverse polarity of both side of the velocity flow and resemble the well-known FAC region 1 and 2 picture by Iijima and Potemra (1976) in the Earth's magnetophere that emerges under certain velocity parameters.

In the second case ($V_0 = 0$, and $V_0' \neq 0$) we again seek localized solutions. The following φ_1 - A_1 relation however holds

$$2(\varphi_1 + V_0'x^2 + u^2 / V_0') = V_0'(A1 - B_\perp x)^2 / B_\perp{}^2 \tag{20}$$

Structures of smaller spatial scales in comparison to the external velocity gradient scales are inferred. The greater the velocity gradients are, the greater the induced FAC intensity is. Figure 1 and 2 illustrate quadrupole structure and its complication (an octopole structure).

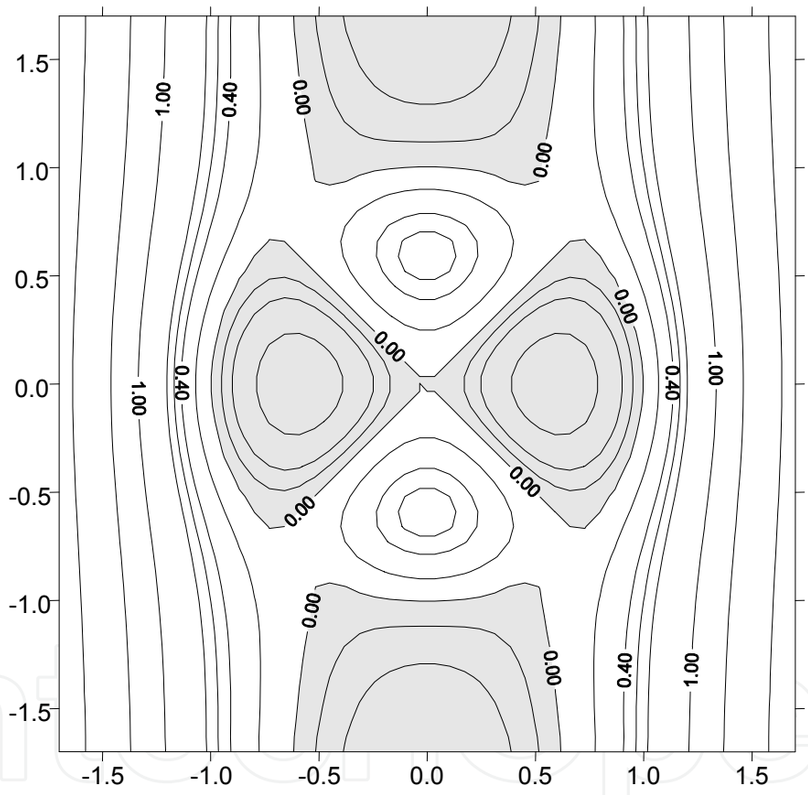

Fig. 1. Example of FAC qadrupole structure in a flux tube of dimensionless radius 1 immersed in shear velocity flow (V_0=0, $V_0' \neq 0$). Hatched and non-hatched area denotes FAC and vortex structures of opposite sign.

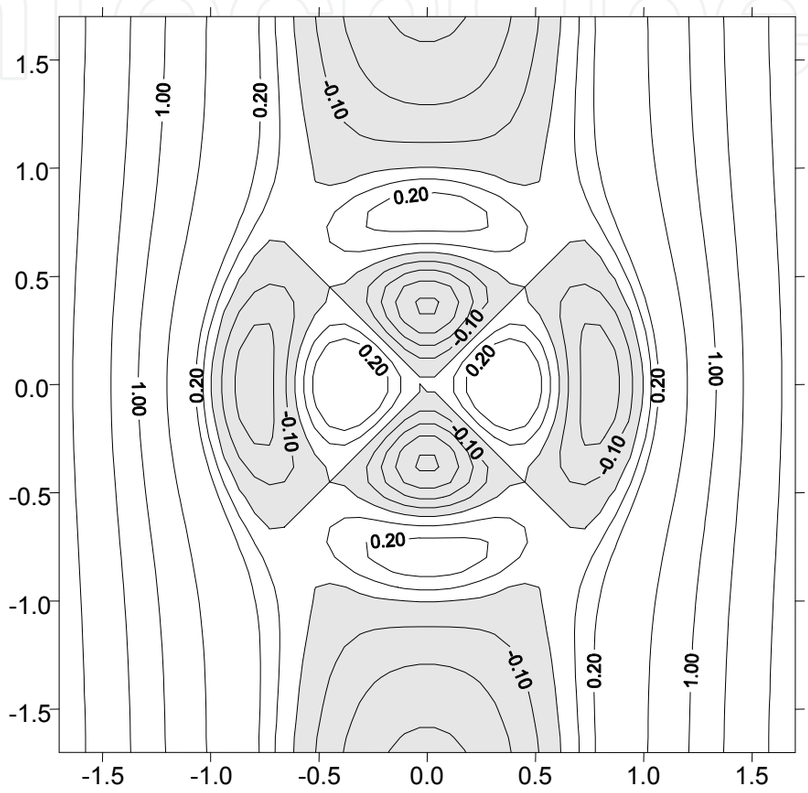

Fig. 2. Example of FAC octopole structure in a flux tube of radius 1 immersed in shear velocity flow (V_0=0, $V_0' \neq 0$). Hatched and non-hatched area denotes FAC and vortex structures of opposite sign.

Further complications are expected under simultaneous considerations of V_0 and V_0'. Both factors suffice to yield more complex structures. The magnetic field variations in the radius r which govern the FAC localization supported by such filaments are illustrated in Figures 3 and 4. We note that transition filaments (e.g. a mixture of dipole and quadrupole structures) arise.

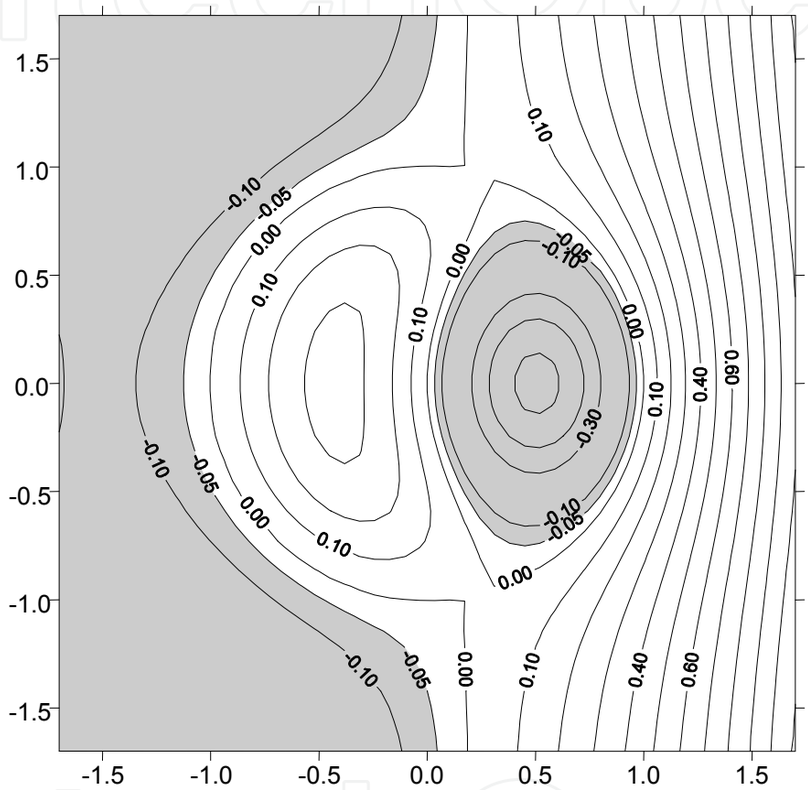

Fig. 3. FAC vortex/thread structures under inhomogeneous flow conditions for $V_0' r_0/V_0$ = 0.08. Hatched and non-hatched area denotes FAC and vortex structures of opposite sign.

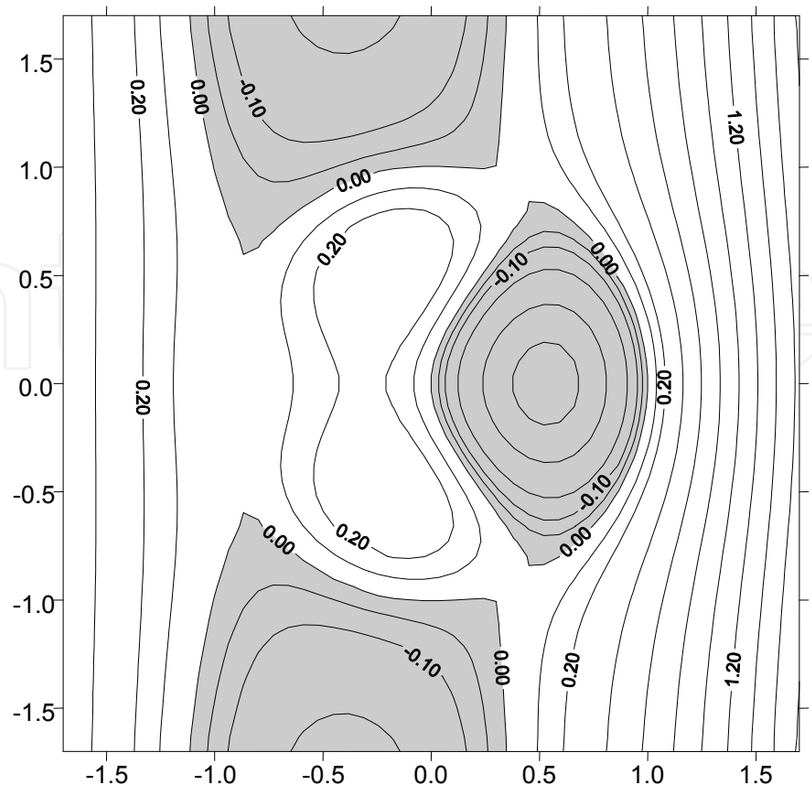

Fig. 4. FAC vortex/thread structures under inhomogeneous flow conditions. $V_0' r_0/V_0 = 0.2$. Hatched and non-hatched area denotes FAC and vortex structures of opposite sign.

The transitional forms are: modified dipole structure and three-cell structure. The three-cell structure consists of a cell (filament) of intense plasma motion and intense FAC, and two weakened cells of equal polarity which are partly connected.

2.4.2 Filament (sub)structures or threads

The above results show that the structures complicate with increasing the inhomogeneity effects, i.e. by including next derivatives (V_0'', V_0''', etc.). There are considerations that the inclusion of odd-number derivatives only would give to one twisted thread of smaller size enveloping the flux tube z-axis. The structure modes examined here are presumably generated by velocity and velocity shear motion in the photosphere under or adjacent to the arch-shaped or loop QP footpoints. The velocity itself and its gradients at the chromosphere level could considerably influence the structure evolution.

Now we arrive closer to possible sources for the structures formation/destabilization processes in the solar atmosphere. The effect comes from the possibility the field-aligned currents to be intensified by filamentation processes. Another possible mechanism is the feeding of the field-aligned currents at the chromosphere) (Nenovski et al, 2001). This feeding enhances the filament velocity/magnetic field gradients and vice versa. The magnitude of the perpendicular component of the magnetic field increases and the pitch angle ϑ increases, as well. As a consequence, a QP (flux tube) destabilization due to filament FAC intensification processes may result.

2.5 Joule heating

The main factors that change the conditions of FAC structure generation and their dynamical evolution approaching the chromosphere heights are the indispensable intensification of the large-scale field-aligned current system and the transition from high to low β plasma conditions along their propagation direction. FAC filament formation processes might appear. The latter could facilitate drastically the FAC structures of different scales that will appear under appropriate FAC threshold values. The FAC filament formation expected at heights above the chromosphere would be the most favorable mechanism of FAC instability and subsequent enhanced (Joule) dissipation at the chromosphere heights.

The Joule heating is due to the Pedersen current and has been already described (e.g. Rees et. al., 1983). Its connection with the FAC distribution $j_{||}$ is given by

$$j_{||} = -\nabla \cdot \vec{J}_{chromo} = -\nabla \cdot (\Sigma_P \vec{E} + \Sigma_H \vec{B} \times \vec{E}) \tag{21}$$

where

$$\vec{J}_{chromo} = \int dz j_{chromo}$$

Σ_P and Σ_H are the Pedersen and Hall conductances (integrated along z Pedersen and Hall conductivities), $\boldsymbol{E}$ is the electric field strength. The electromagnetic energy dissipation in the chromosphere (treated as a resistance) is thus

$$Q = \Sigma_P E^2 \tag{22}$$

The temperature increase, ΔT, connected with the dissipation rate Q is determined by

$$Q = C_p \Delta T \tag{23}$$

where Cp is the heat capacity of the medium. The latter is dependent on the neutral (hydrogen) density N_n distribution in height. At chromosphere heights the proton drift/electric field distribution might still be considered in frozen field condition, i.e. the electric field $\boldsymbol{E}$ is dependent on the plasma drift and the ambient magnetic field. This means that knowing the Pedersen conductivity σ_P and the ion drift $\boldsymbol{V}$ at the given height the temperature change ΔT (that depends on the Joule heating mechanism) might be determined.

At which heights are the greatest changes in the proton temperature ΔT expected? Let us model the profile of the temperature change ΔT using the chromosphere density, the Pedersen conductivity and the proton-neutral collision frequency distribution in height. The Pedersen conductivity σ_P is given by

$$\sigma_P = Ne^2 \left(\frac{\nu_{pn}}{\nu_{pn}^2 + \omega_{cp}^2} + \frac{\nu_e}{\nu_e^2 + \omega_{ce}^2} \right)$$

where N is the chromosphere density concentration, ν_{pn} and ν_e are the proton-neutral and electron collision frequencies, ω_{cp} and ω_{ce} are the proton and electron cyclotron frequencies.

At heights where the cyclotron frequencies are greater than corresponding collision frequencies, the Pedersen conductance is proportional to

$$\sigma_P \cong Ne^2\left(\frac{\nu_{pn}}{\nu_{pn}^2+\omega_{cp}^2}\right) \cong Ne^2\frac{\nu_{pn}}{\omega_{cp}^2}$$

Having in mind that proton collision frequency ν_{pn} is determined by the density N_{n} and the proton temperature T_{p}, and that the heat capacity Cp is proportional also to N_{n}, the temperature change ΔT at given height z is thus given by:

$$\Delta T(z) \equiv Q(z)/C_p(z) = \sigma_P(z)E^2/C_p(z) \propto NT_p\,. \tag{24}$$

The latter result suggests that the temperature changes follow the plasma density changes at least at heights where the Pedersen conductivity approximation is applicable. This certainly includes the chromosphere-corona transition heights. The above considerations suggest that the Joule heating depending on the FAC geometry and intensity, should result both in horizontal and vertical distributions. Thus, both the observable FAC intensity distribution (plasma vortex) and the ion temperature changes in heights might be used as benchmarks of the QP destabilization mechanisms.

The overall dissipation rate is thus proportional to the squared field-aligned current density $j_{\|}$ multiplied by squared factor F:

$$W_{diss} \geq (j_{\|,crit}F)^2/\sigma_P \tag{25}$$

at heights where Pedersen conductivity σ_{P} is different from zero. It follows that the FAC dissipation steepens with the decrease of the FAC scale. It is concluded that the dissipation and subsequent heating events are much more effective in the finest FAC structures expected in thread-like QP configurations. An increase of dissipation accompanied with temperature increase *however* might oppose the FAC filamentation process due to a temperature increase (the threshold values (eq. 16) subsequently increase). It is suggested that FAC filamentation and associated heating events are therefore counteracting processes and the both processes represent an essential component of QP destabilization mechanisms. If the QP destabilization event occurs, this leads to a subsequent generation of solar wind and/or coronal mass ejection (CME) events.

3. Conclusion

The MHD structure and wave generation is thought to be among the various processes initiated by the photospheric MHD disturbances, which propagate upward through the QP feet. We propose here a possible way of generating FAC (sub)structures in an arch-type QP by the MHD approach.

An emergence of FAC structures due to interactions of field-aligned current elements (subunits) that form the whole FAC system itself is demonstrated theoretically. We used the charge concept to build 'charge' counterparts responsible for the FAC filament formation mechanism. At some specific value of the control parameter, $\lambda^2 \equiv \mu_0(j_{\|})^2/N_0\Theta$, these FAC elements bifurcate in new stationary states. Thus, a hierarchy of threshold value values for the

emergence of FAC structures of different scales is derived. We demonstrated that the FAC structure formation appears as a counterpart of the pinching effect. Another difference is a co-existence of FAC structures of different scales that is possible above the threshold values. This FAC filament formation is considered in the term of successive stationary states that would evolve at the end to enhanced FAC dissipation. It is found that the threshold value for an initiation of the FAC structure formation depends on the plasma 'thermal' velocity and it is easily attainable for low β plasma conditions just above the chromosphere. The stationary FAC structures examined thus are an appropriate modelling of the dynamical transition of both the plasma and FAC vortex/thread structures from their initial states toward new ones during their journey through the chromosphere-corona transition regions.

The relevance of our problem of the FAC structure formation to the MHD point of view is pointed out, as well. In the Grad-Shafranov theory of the magnetohydrodynamic equilbria problem the stream function equation for the steady two-dimensional flow of non-viscous plasmas is exploited. It will therefore govern stationary (equilibrium) magnetohydrodynamic structures. A comparison shows the identity of the two equations and grounds our 'charge concept' approach with the magnetohydrodynamic equilibria problem. Our 'charge concept' approach determines quantitatively the nonlinearity coefficient, i.e. $\lambda^2 \equiv \mu_0(j_\parallel)^2/N_0\Theta$. Note that in previously developed inertial/kinetic Alfven wave models (e.g. Chmyrev et al., 1988, Knudsen, 1996) this nonlinearity coefficient (denoted there by k^{-1}) corresponds to the squared plasma electron inertia c/ω_{pe} being dependent on plasma density only. In contrast to the above-mentioned inertial/kinetic Alfven wave model, our general examination states that FAC/vortex/tread structures will be controlled by the β plasma parameter and hence, FAC structure formation process will emerge at heights sufficiently close to the chromosphere, or just above it.

A simple physical analogue of magnetic flux tube immersed in plasma flow and generation of threads/filaments and their basic characteristics are examined, as well. The analogue consists of plasma flow velocity, velocity and magnetic field gradients, and sectors with non-zero azimuthal magnetic fields. This allows to making a 2-D model of the plasma circulation and the pitch angle evidence of the twisted magnetic field lines in flux rope models of the prominence threads. The velocity and the magnetic fields dependence on the distance x is of power law character. Structure organization and thread formation processes are studied on the basis of ideal MHD equation set. In the case of power law degree greater than one the vortices whose number depends on that degree are intermixed and various threads regimes along the axial magnetic field could be established. An example of one flux rope could be constructed in the limit of infinite series of odd power law-dependent velocity. A quadrupole flux rope which consists of four nearly distinct threads is formed in the simplest case of linear x-dependence. Field-aligned currents of the threads responsible for growing of the pitch-angle and for diminishing of the magnetic field tension are allowed for. The analytical and numerical results could be applied to solar prominence structure evolution and destabilization processes.

In summary, two factors responsible for structure formation processes in flux tubes: field-aligned current self-interaction and interaction with external plasma flow are taken into account. The following results would be inferred:

First, FAC filamentation process due to self-interaction process starts at certain threshold values of the FAC density in the prominence body. Changes of FAC intensity and the

plasma parameter β along the magnetic field fluxes will control FAC structure formation processes. Preferable conditions for the examined FAC filament formation processes are met at heights approaching the chromosphere-corona transition region;

Second, flux tubes immersed in plasma flow are exposed to structure changes, as well. Factors responsible for structure formation of flux tube (visible in H_α line and other optical devices) are the flow velocity itself and velocity gradients;

Third, in the field of uniform plasma flow with velocity V_0 six-sheet FAC structures are easily formed. Note that such structures are evidenced in the Earth's magnetosphere (the FAC region 1 (R1) and 2 (R2) discovered by Iijima and Potemra (Iijima and Potemra, 1976);

Fourth, flow velocity gradient (a linear x-dependent velocity) causes quadrupole (octopole) structures. Their scales are of smaller sizes than the corresponding velocity gradient scale;

Fifth, flow velocity and the velocity shear results in structure complication. Transitional forms (e.g. modified dipole, three-cell, etc) could be generated.

Our theoretical results refer to the most simplified models of prominence structure destabilization. We consider FAC intensification process as basic QP destabilization mechanisms due to active chromosphere processes - the plasma density, velocity and/or conductivity enhancements.

The obtained criteria for QP destabilization are suitable for observational verification of the proposed mechanism of FAC filament and thread generation. Detailed examinations of all the plasma parameters and characteristics in the quiescent prominence body and experimental evidences are further needed.

4. Appendix A

1. *Characteristic time scales*. It is well known that the highest characteristic frequency associated with collective modes in non-magnetized plasmas is the electron plasma frequency

$$\omega_{pe} = (4\pi N e^2/m_e)^{1/2}. \tag{A1}$$

In a system where the main effects come from the ambient magnetic field the Lorentz force is the dominant component. Should a flow change, say Δv appear particles of mass m and charge q in a first approximation respond to the Lorentz force

$$m\mathrm{d}\Delta\boldsymbol{v}/\mathrm{d}t = \Delta\boldsymbol{F} \approx q\,\Delta\boldsymbol{v}\times\boldsymbol{B}_0, \tag{A2}$$

where $\Delta\boldsymbol{v}$ is the disturbance flow velocity. From (A2) it follows that such a disturbance will grow with a growth rate

$$\gamma \approx qB_0/m = \omega_c. \tag{A3}$$

Thus, in an ensemble of charged particles immersed in strong ambient magnetic field $\boldsymbol{B}_0$ another characteristic time of collective processes equal to the cyclotron frequency $\omega_{c\alpha} = q_\alpha B_0/m_\alpha$ appears (α denotes the charged particle $\alpha = e,i$). The characteristic velocity of propagation of (electric) forces in magnetized plasmas is the Alfven velocity v_A expressed by $B_0/(\mu_0\rho_0)^{1/2}$, where ρ_0 is the plasma density. In term of above-mentioned

characteristic frequencies, the Alfven velocity is equal to $(\omega_{ci}/\omega_{pi})c$, where c is the light speed, i.e. the characteristic velocity is modified by the ω_{ci}/ω_{pi} ratio. In plasmas where FAC structures of size d exist there is another time scale t_{FAC} equal to $d/v\mathbf{A}$. Therefore, *collective* plasma behavior is only observed on time-scales longer than the $\omega_{p\alpha}^{-1}$, $\omega_{c\alpha}^{-1}$ and/or t_{FAC}.

Let us now estimate time scales for FAC filament formation process in the chromospere-solar corona system. At heights close to the chromosphere the ambient magnetic field B_0 is approximately equal to 1-20 G, or less. The plasma number density is ~3-6x10^{17} m^{-3} and decreases slowly. The cross size d of ambient FACs is usually about 10^3 km and less and should increase in height. Taking it into account and using (A1) and (A3) we obtain that at chromospheric heights the greatest time scale equals to $t_{FAC} \approx 10^2$ s. Thus, we conclude that in the worst case the characteristic time of collective processes as FAC filament formation is less than of a minute. On the other hand, the FAC structures propagate to the chromosphere with the Alfven velocity v_A. Then the propagation time depends on the distance between the cromosphere and the region where the FAC filament formation appears. It equals from seconds to minutes. Fortunately, the time-scale for evolution of FAC structures treated by us is much less than that across the prominence body. Thus, the dynamics of Alfvén (shear and compressional) waves in such a dynamics can be neglected in zeroth order approximation.

2. *Condition for FAC closure through the chromosphere*. In the process of FAC structuring however the FAC intensity required for it increases inversely proportional to the FAC structure scale a. This means than FAC of smaller scales have higher intensities. The following question could arise: whether chromospheres can close prominence FAC structures whatever scale it is of.

   The FAC intensity, or $j_{||}$ is closed through the chromosphere by the Pedersen and Hall currents provided that

$$j_{||} = j_{||,\,\mathrm{chromo}} \equiv \boldsymbol{\nabla}.\boldsymbol{J}_{\perp,\,\mathrm{chromo}} \tag{A4}$$

   The perpendicular current $\boldsymbol{J}_{\perp,\,\mathrm{chromo}}$ is given by:

$$\boldsymbol{J}_{\perp,\,\mathrm{chromo}} = \Sigma_P\boldsymbol{E} + \Sigma_H(\boldsymbol{B}_0 \times \boldsymbol{E}) \tag{A5}$$

   where Σ_P and Σ_H are the Pedersen and Hall conductances evaluated in height. They are assumed to be almost homogeneous in horizontal direction. Then (A4) becomes

$$j_{||,\,\mathrm{chromo}} = \boldsymbol{\nabla}.[\Sigma_P\boldsymbol{E} + \Sigma_H(\boldsymbol{B}_0 \times \boldsymbol{E})] \cong \Sigma_P\,\boldsymbol{\nabla}.\boldsymbol{E} - \Sigma_H\boldsymbol{B}_0(\boldsymbol{\nabla}\times\boldsymbol{E}) = -\Sigma_P\ \boldsymbol{\nabla}.(\boldsymbol{v}\times\boldsymbol{B}_0). \tag{A6}$$

   where the $\nabla\times E$ part is considered to be zero (electrostatic field approximation). In the solar corona the (convection) electric field E is determined by the non-collisional Ohm's law $\boldsymbol{E} + \boldsymbol{v}\times\boldsymbol{B}_0 = 0$. Under the condition of equipotentiality of the magnetic field tubes both the electric field and the corresponding fluid velocity v enter the chromosphere region. The following relationship between the fluid velocity v and the magnetic field disturbance b produced by FAC comes from the corona region:

$$b = (B_0/v_A)v, \tag{A7}$$

   where v_A is the Alfven velocity. It is a consequence from the well-known Walen relation (in magnetohydrodynamics). Using the Maxwell equation

$$\nabla \times \boldsymbol{b} = \mu_0 \boldsymbol{j} \tag{A8}$$

where the displacement current $\partial E/\partial t$ is conventionally neglected we obtain for its parallel component:

$$(B_0/v_A)\Omega = \mu_0 j_{||} \tag{A9}$$

where factor (B_0/v_A) is assumed to vary along the ambient magnetic field direction $\boldsymbol{B}_0/B_0$ only, i.e. it is homogeneous in horizontal direction. By a comparison of (A4) and (A6) the condition for FAC closing through the chromosphere, $j_{||,\,\mathrm{chromo}} \geq j_{||}$, results in the following inequality

$$\Sigma_P \geq (\mu_0 v_A)^{-1} \equiv \Sigma_W. \tag{A10}$$

where Σ_W is the wave conductance. In practice, such magnitudes of the Pedersen conductance are frequently observed (Nenovski et al, 2001). Hence, irrespectively of the FAC intensity, the FAC closure condition through the chromosphere will be controlled by the Pedersen conductance magnitude.

The chromosphere itself will however not be simply a passive recipient of the field-aligned currents. The FAC can modify the chromospheric conductivity by ionising the neutral photosphere, producing additional electron-proton pairs due to particle fluxes permeating the chromospere-photosphere system. In the presence of a background electric field $\boldsymbol{E}$, the conductivity gradients produced by particles can lead to divergences in the perpendicular chromospheric currents, which in turn lead to additional parallel field-aligned currents.

5. References

Arshinkov, I., Bochev, A., Nenovski, P., Marinov, P., and Todorieva, L. (1985) *Adv. Space Res*. 5, 127-130.

Balescu, R. (1975) *Equilbrium and nonequilibrium statistical mechanics*, John Wiley, N.Y., ch. 6, 11.

Bellan, P. M.(2004) Final Technical Report for DOE Grant DE-FG03-97ER54438, Applied Physics, Caltech, Pasadena CA 91125, December 21.

Ballester, J. L., & Priest, E. R. 1989, A&A, 225, 213

Bashkirtsev, V., Kobanov, N., & Mashnich, G. 1983, Solar Phys., 82, 443

Bashkirtsev, V., & Mashnich, G. 1984, Solar Phys., 91, 93

Bennett, W.H. (1934) *Phys. Rev*. 45, 890-897.

Bommier, V., Leroy, J.-L., & Sahal-Brechot, S. 1986, A&A, 156, 79

Chmyrev, V.M., Bilichenko, S.V., Pokhotelov, O.A., Marchenko, V.A., Lazarev, V.I., Streltsov, A.V., and Stenflo, L. (1988) *Physica Scripta*, 38, 841-854.

Christon, S.P., Mitchell, D.G., Williams, D.J., Frank, L.A., Huang, C.Y. and Eastman, T.E. (1988) *J.Geophys. Res.* 93, 2562-2572.

Cui Shu, Hu Ju, Ji Guo-Ping, et al. 1985, Chin. A&A, 9, 49

Ecker, G. (1972) *Theory of fully ionized plasmas* (Academic press, New York)

Engvold, O. 1976, Solar Phys., 49, 238

Hirayama, T. 1986, in NASA CP-2442, Coronal and Prominence Plasmas, ed. A. I. Poland, 149

Hirayama, T., Nakagomi, Y., & Okamoto, T. 1979, in Phys. Solar Prominences, ed. E. Jensen, P. Maltby, & F. Q. Orrall, IAU Coll. 44, 48
Hirayama, T. 1971, Solar Phys., 17, 50
Hirayama, T. 1972, Solar Phys., 24, 310
Hirayama, T. 1985a, Solar Phys., 100, 415
Hirayama, T. 1985b, in Dyn. Quiescent Prominences, ed. V. Ruzdjak, & E. Tandberg-Hanssen, IAU Coll., 117, 187.
Iijima, T. and Potemra, T.A. (1976) *J. Geophys. Res.* 81, 2165-, 5971-.
Kaptsov, O.V. (1988) *Dokl. Akad.Nauk SSSR* 298, 597-600.
Knudsen, D.J. (1996) *J. Geophys. Res.* 101, 10 761-10772.
Kubot, J. 1980, in ed. A. F. Moriyama, & J. C. Henoux, Proc. Japan - France Seminar on Solar Physics, 178
Landman, D. A. 1984a, ApJ, 279, 183
Landman, D. A. 1984b, ApJ, 279, 438.
Leroy, J.-L. 1985, in NASA Conf. Publ. 2374, Measurements of Solar Vector Magnetic Fields, ed. M. J. Hagyard, 121
Lin, Y., Engvold, O., & Wiik, J. E. 2003, Sol. Phys., 216, 109;
Lin, Y. 2004, Ph.D. thesis, Univ. Oslo
Lin, Y., Engvold, O., Rouppe van der Voort, L. H. M., Wiik, J. E., & Berger, T. E. 2005, Sol. Phys., 226, 239
Lin, Y., Engvold, O., Rouppe van der Voort, L. H. M., & van Noort, M. 2007, Sol. Phys., 246, 65.
Malherbe, J. M., Schmieder, B., Ribes, E., & Mein, P. 1983, A&A, 119, 197
Martinov, N, Ourushev, D. and Georgiev, M. (1984) *J. Phys*. C 17, 5175-5184.
Martinov, N., Ourushev, D. and Chelebiev, E. (1986) J. *Phys. A: Math. Gen*. 19, 1327-1332.
Mein, P., & Mein, N. 1991, Solar Phys., 136, 317
Mein, P. 1977, Solar Phys., 54, 45
Ohtani, S., Zanetti, L.J., Potemra, T.A., Baker, K.B., Ruohoniemi. J.M., and Lui, A.T.Y. (1994) *Geophys. Res. Lett.* 21, 1879-1882.
Nenovski, P. (1996) *Phys. Scripta* 53, 345-350.
Nenovski, P., Dermendjiev, V. N., Detchev, M., Vial, J.-C and Bocchialini, K.(2001) On a mechanism of intensification of field-aligned currents at the soalr chromospere-quiescent prominence boundaries, Astronomy & Astrophysics, 375, p.1065-1074.
Nenovski, P.,Danov, D. and Bochev, A. (2003) On the field-aligned current filament formation in the magnetospere, J. Atm. Solar-Terr. Phys., 65, pp 1369-1383.
Nenovski, P. (2008) Comparison of simulated and observed large-scale, field-aligned current structures, Annales Geophysicae, 26, pp. 281-293
Nezlin, M.,Rulov A., Snezhkin E. N., Trubnikov A. S., (1987) Self-organizaion of spiral-vortex structures in shallow water with repid differenial rotation, Sov.Phys.JETP, v.65(1), pp.1-4.
Nezlin, M., Snezhkin E. N. (1993) Rossby Vortices, Spiral Structures, Solitons, Springer-Verlag, Berlin, Heidelberg.
Nezlin, M.V. (1994) Modeling of the Generation of Spiral Structure by Laboratory Experiments in Rotating Shallow Water, and Prediction of Interarm Anticyclones in Galaxies, In Proc. "Physics of the Gaseous and Stellar Disks of the Galaxy", SAO,

22-25 September 1993, Russia, ed. I.R.King, ASP Conference Series, 66, pp. 135-151, 1994.
Oliver, R. 1999, in ESA SP-448, Magnetic Fields and Solar Processes, ed. A. Wilson (Florence, Italy), 425
Northrup, E.F. (1907) Phys. Rev. 24 474 (1907).
Parker, E.N. (1979) *Cosmical magnetic fields. their origin and their activity*, Clarendon Press, Oxford, Vol.1, ch. 4
Sato, T. (1982) in *Magnetospheric Plasma Physics*, Reidel, Tokyo, ch. 4.
Schmieder, B., Malherbe, J. M., Mein, P., & Tandberg-Hanssen, E. 1984, A&A, 136, 81
Schmieder, B., Malherbe, J. M., Poland, A. I., & Simon, G. 1985, A&A, 153, 64
Shafranov, V.D. (1963) Ravnovecie plasmy v magnitnom pole, in *Voprocy teorii plasmy*(in russian), Atomizdat, Moscow, Vol.2, 92-176.
Shkarofsky, I.P., Johnston, T.W., and Bachynski, M.P. (1966) *The particle kinetics of plasmas*, Addison-Wesley, Reading, Massachusetts, ch.10.
Southwood, D.J. and Kivelson, M.G. (1993) *Adv. Space Res*. 13, No 4, (4)149-(4)157.
Speiser, T.W. (1965) *J. Geophys. Res*. 70, 4219-4226.
Speiser, T.W. (1967) *J. Geophys. Res*. 72, 3919-3932.
Stenflo J.O., (1976) Basic Mechanism of Solar Activity, Proc.IAU Symp. 7.1, Reidel, Dordrecht.
Strauss, H.R.(1977) Phys. Fluids, 19, 134, 1976; 20, 1354,
Streltsov, A.V., Chmyrev, V.M., Pokhotelov, O.A., Marchenko, V.A. and Stenflo, L (1990) *Physica Scripta*, 41, 686-692.
Tsubaki, T., & Takeuchi, A. 1986, Solar Phys., 104, 313
Tsubaki, T., Toyoda, M., Suematsu, Y., & Gamboa, G. 1988, PASJ, 40, 121
Tsubaki, T. 1989, in Solar and Stellar Coronal Structures and Dynamics, National Solar Observatory, ed. R. C. Altrock, 140
Vernazza, J. E., Avertt, E. H., & Loeser, R. 1981, ApJS, 45, 635
Vial, J.-C. 1982, ApJ, 253, 330
Vial, J.-C. 1986, in ed. A. I. Poland, NASA CP-2442, Coronal and Prominence Plasmas, 89
Vrsnak, B. 1993, Hvar Obs. Bull., 17, 23
Vrsnak, B., & Ruzdjak, V. 1994, in Solar Coronal Structures (VEDA Publ. House, Tatranska Lomnica), ed. V. Rusin, P. Heinzel, & J.-C. Vial, IAU Coll., 144,
Yi, Z., & Engvold, O. 1991, Sol. Phys., 134, 275
Yi, Z., Engvold, O., & Keil, S. 1991, Solar Phys., 132, 63
Wu, S.T., Hu, Y.Q., Nakagawa, Y., and Tandberg-Hanssen, E., Induced mass and wave motions in the solar atmosphere. I. Effects of shear motion of flux tubes, The Astrophys. J., 266 (1983) 866-881.
Zhang, Q. Z., Livingston, W. C., Hu, J., & Fang, C. 1987, Solar Phys., 114, 245 Zirin, H., & Severny, A. B. 1961, Observatory, 81, 155
Zirker, J. B., Engvold, O., & Martin, S. F. 1998, Nature, 396, 440

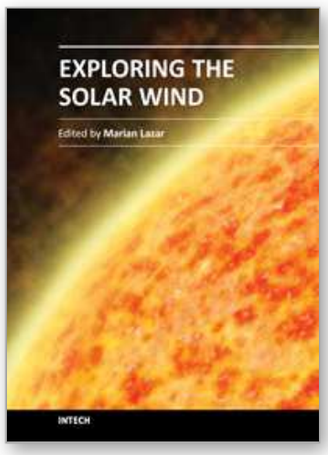

Exploring the Solar Wind

Edited by Dr. Marian Lazar

ISBN 978-953-51-0339-4
Hard cover, 462 pages
Publisher InTech
Published online 21, March, 2012
Published in print edition March, 2012

This book consists of a selection of original papers of the leading scientists in the fields of Space and Planetary Physics, Solar and Space Plasma Physics with important contributions to the theory, modeling and experimental techniques of the solar wind exploration. Its purpose is to provide the means for interested readers to become familiar with the current knowledge of the solar wind formation and elemental composition, the interplanetary dynamical evolution and acceleration of the charged plasma particles, and the guiding magnetic field that connects to the magnetospheric field lines and adjusts the effects of the solar wind on Earth. I am convinced that most of the research scientists actively working in these fields will find in this book many new and interesting ideas.

INTECH
open science | open minds

InTech Europe
University Campus STeP Ri
Slavka Krautzeka 83/A
51000 Rijeka, Croatia
Phone: +385 (51) 770 447
Fax: +385 (51) 686 166
www.intechopen.com

InTech China
Unit 405, Office Block, Hotel Equatorial Shanghai
No.65, Yan An Road (West), Shanghai, 200040, China
中国上海市延安西路65号上海国际贵都大饭店办公楼405单元
Phone: +86-21-62489820
Fax: +86-21-62489821

IntechOpen